Observation of the Taylor instability in a dusty plasma

K. A. Pacha, J. R. Heinrich, S-H. Kim, and R. L. Merlino[a)]

Department of Physics and Astronomy

The University of Iowa, Iowa City IA 52242

Submitted as a Brief Communication to Physics of Plasmas
(September 20, 2011)

ABSTRACT

Observations of the Taylor instability in a laboratory dusty plasma are presented. The dust cloud, formed in a dc argon glow-discharge plasma, is stratified into regions of high and low dust densities. The instability was triggered by a spontaneous intrusion of the low density dust fluid into the high density dust fluid at the interface. The instability in the dust fluid was phenomenologically similar to the hydrodynamic Taylor instability that occurs when a light fluid is accelerated into a heavy fluid.

PACS Numbers: 52.27.Lw, 47.20.Ma, 52.35.Py

[a)] Electronic Mail: robert-merlino@uiowa.edu

The Taylor instability (TI) is an instability at the interface between two fluids of different densities that occurs if the low density fluid is accelerated into the high density fluid.[1] It is a generalization of the instability, analyzed by Lord Rayleigh, that develops if a heavy fluid is superposed on a light fluid in a gravitational field.[2] The general feature of the Rayleigh-Taylor instability (RTI) is the growth of interfacial protuberances ('bubbles' and 'spikes').[3] In this Brief Communication, we present observations of the TI in a dusty plasma. Dusty plasmas can exist in a broad range of states from crystalline to fluid. When the rate of momentum exchange due to dust-dust electrostatic interactions exceeds that of other interactions, a dusty plasma can be considered essentially as a one-phase (i.e., fluid) system, and can be used to study hydrodynamical instabilities.[4] The RTI has been invoked to explain certain fluid-like behavior observed in an rf-produced dusty plasma.[5]

The observations were made in the device shown in Fig. 1. A glow discharge in argon at a pressure, P = 140 mTorr (19 Pa), was formed by applying a positive bias of 300 V (discharge current = 23 mA) to a 3.6 cm diameter anode disk with respect to the grounded walls of a large cylindrical (0.6 m diam. by 1 m length) vacuum chamber. An axial magnetic field (3 mT) confined the electrons, so that an elongated anode glow was formed along the magnetic field direction. Dust particles located on a floating tray below the anode become negatively charged and incorporated into the discharge. The confinement of the dust particles in anodic glows has been described by Trottenberg *et al*.[6] Spherical iron particles, with diameters in the range of 1 – 5 μm were used in these experiments, although similar observations were made using other types and sizes of dust particles. The dust particles were illuminated by a thin vertical sheet of 432 nm laser light and were imaged using a CCD camera at 30 Hz. The intensity of the scattered light is proportional to the dust density. Typical plasma and dust parameters were: electron and ion temperatures, $T_e = 100\ T_i = 2.5$ eV, ion density, $n_i \sim 10^{14}$ m^{-3}, dust density, $n_d \sim 10^{10}$ m^{-3}, and dust charge $eZ_d \sim 2000 – 10{,}000$. Further details of the experimental set-up can be found in ref. 7.

A single-frame image of a 2 mm vertical slice through the center of the dust cloud is shown in Fig. 2(a). The anode is visible on the right side of this photo. The dust cloud has a conical shape, with a dense region near the anode and a rarefied region farther from the anode. The boundary of the dust suspension is indicated by the dotted curve. A profile of

the scattered light intensity (~ dust density) within the box in Fig. 2(a) is shown in Fig. 2(b). Since the instability occurred on the front boundary of the dense portion of the cloud (position ≈ 22 mm), the laser intensity and camera aperture were adjusted so that the pixel intensities in the image of the dense portion of the cloud, were not saturated.

The development of the instability is shown in Fig. 3 in a montage of eight consecutive single-frame video images recorded at 1/30 s intervals. (A video showing several examples of the instability is available in the enhanced online material.) The instability was excited at the location indicated by the arrow in Fig 3(a), when a small ripple spontaneously appeared on the front side of the dense dust region. This initial perturbation grew rapidly into a wedge-shaped bubble that penetrated into the dense dust fluid [Figs. 3(b) and (c)]. In Fig. 3(d) a spike of dense fluid can be seen projecting back into the bubble. As the spike evolved it rolled up into a vortex-like structure [Fig. 3(e) – (g)], and eventually coalesced with the bubble [Fig. 3(h)]. Although it is not apparent in the single frame images, the video record showed that the bubble and spike were convected upward (bottom to top in Fig. 3) as they developed. This upward motion occurred at a speed ~ 2–3 cm/s, and was part of the overall convective flow of the dust suspension, most likely due to a combination of electric and ion drag forces on the fluid. When the bubble and spike moved upward by a sufficient amount, the segment of the boundary where the initial perturbation occurred returned to a stable state until the next disturbance appeared and the instability occurred again. The disturbances did not occur with a regular frequency, but typically were separated by 0.4—0.7 s time intervals.

The evolution of the bubble and spike was studied by plotting the scattered light intensity within the rectangle shown in Fig. 3(b). The results in Fig. 4 show the penetration of the bubble (t = 0 to t = 0.2 s) into the dense fluid, followed at t = 0.27 s, by the appearance of a spike of dense fluid pushing back into the bubble (t = 0.27 s to t = 0.3 s), toward the initial unperturbed boundary. At t = 0.3 s, the spike had expanded, filling the bubble and restoring the initial boundary. The amplitude of the instability was obtained from measurements of the area of the bubble, A_b, using $A_b^{1/2}$ as an indicator of the amplitude. A plot of $A_b^{1/2}$ vs. time for seven separate instability episodes is shown in Fig. 5. Although there were variations from episode to episode, each occurrence showed the same

general trend of bubble formation and growth lasting about 0.2 s, followed by the appearance of the spike pushing back into the bubble.

The development of the observed instability is similar to that described by Sharp[3] for a Taylor unstable interface between two *incompressible* liquids. Within a single video frame (1/30 s) of its appearance, the ripple penetrated into the dense fluid by an amount comparable to its transverse dimension (wavelength). According to linear theory,[1] the exponential growth of the instability ceases when the size of the disturbance of the interface is no longer small compared with the wavelength. The observations showed that the linear growth phase must have occurred within one video frame (1/30 s). For two semi-infinite *incompressible* fluids of mass densities ρ_1 and $\rho_2 > \rho_1$ separated by a planar boundary and subjected to a sinusoidal perturbation of wavelength λ, the linear growth rate is given $\gamma = \sqrt{(2\pi g'/\lambda) A_T}$, where g' is the acceleration of the light fluid into the heavy fluid, λ is the wavelength of the perturbation, and $A_T = (\rho_2 - \rho_1)/(\rho_2 + \rho_1)$ is the Atwood number.[1] From data in Figs. 2 and 4 we estimate that $g' \sim 900$ mm/s^2, $\lambda \sim 5$ mm, and $A_T \sim 0.8$, so that $\gamma \sim 30$ s^{-1}, which is consistent with the observations. The formation of the bubble and spike is an indication of the nonlinear state of the instability.[3] The roll-up of the spike could be caused by a secondary, shear-driven, Kelvin-Helmholtz instability.

The linear theory of the TI assumes that a sinusoidal perturbation is initially applied to the interface. This, however, is not the situation typically encountered in most cases of practical interest in which the nature of the initial disturbance on the interface is not known. We found that the initial disturbance always seemed to occur at roughly the same location on the interface, which could be related to the curvature of the interface. The segment of the interface where the instability formed was flatter than at other places. A convex surface tends to be more unstable to the TI than a concave one,[8] which could explain why the instability usually started on the flattest part of the interface.

ACKNOWLEGEMENTS

This work was supported by DOE Grant No. DE-FG01-04ER54795.

REFERENCES

1. G. Taylor, Proc. R. Soc. London, Ser. **A 201**, 192-196 (1950).
2. Lord Rayleigh, Proc. London Math. Soc., **14**, 170-177, (1883).
3. D. H. Sharp, Physica **12D**, 3-18 (1984).
4. G. E. Morfill, M. Rubin-Zuzic, H. Rothermel, A. V. Ivlev, B. A. Klumov, H. M. Thomas, and U. Konopka, Phys. Rev. Lett. **92**, 175004 (2004); S. A. Khrapak, A. V. Ivlev, and G. E. Morfill, Phys. Rev. E **70**, 056405 (2004).
5. M. Schwabe, M. Rubin-Zuzic, S. Zhdanov, A. V. Ivlev, H. M. Thomas, and G. E. Morfill, Phys. Rev. Lett. **102**, 255005 (2009).
6. T. Trottenberg, D. Block, and A. Piel, Phys. Plasmas **13**, 042105 (2006).
7. J. R. Heinrich, S.-H. Kim, and R. L. Merlino, Phys. Rev. E, **84**, 026403 (2011).
8. R. Krechetnikov, J. Fluid Mech. **625**, 387-410 (2009).

FIGURE CAPTIONS

FIGURE 1 (color online) Schematic of the experimental set-up.

FIGURE 2 (a) Single-frame video image of the dust cloud. The dotted curve outlines the boundary of the suspension. The bright feature at the back of the dust cloud is due to a spurious reflection. (b) A scan of the scattered light intensity (proportional to the dust density) measured along the rectangular box in (a), showing that the suspension is stratified into low and high density regions.

FIGURE 3 (color online) (a)–(h) Single-frame video images, in 1/30 s intervals, showing the onset and development of the instability on the interface between the low and high density dust fluids. The arrow in (a) indicated the location of the initial perturbation. (b) and (c) The growth and penetration of a bubble. (d) and (e) Growth of the spike. (f) and (g) spike roll-up (indicated by the enlarged dotted curve). (h) Merging of the bubble and spike. (enhanced online) see http://

FIGURE 4 (color online) Scattered light intensity profiles for the rectangular box shown in Fig. 3(b). t = 0 refers to the initial appearance of the ripple on the interface, taken as x = 0.

FIGURE 5 Time history of the bubble amplitude, $A_b^{1/2}$, where A_b is the bubble area, for seven separate occurrences of the instability.

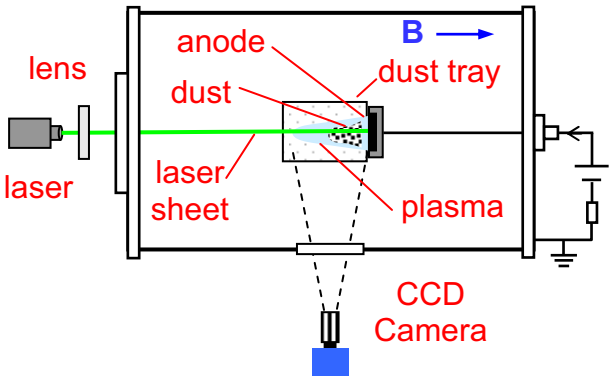
B
anode
lens
dust tray
dust
laser
sheet
plasma
laser
CCD
Camera

Figure 1

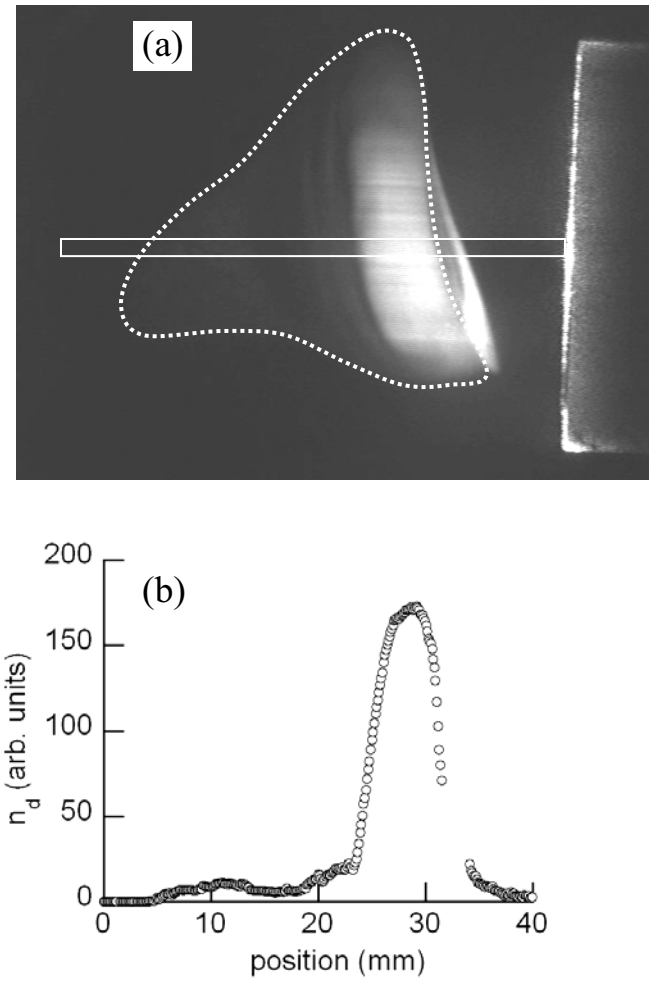

Figure 2

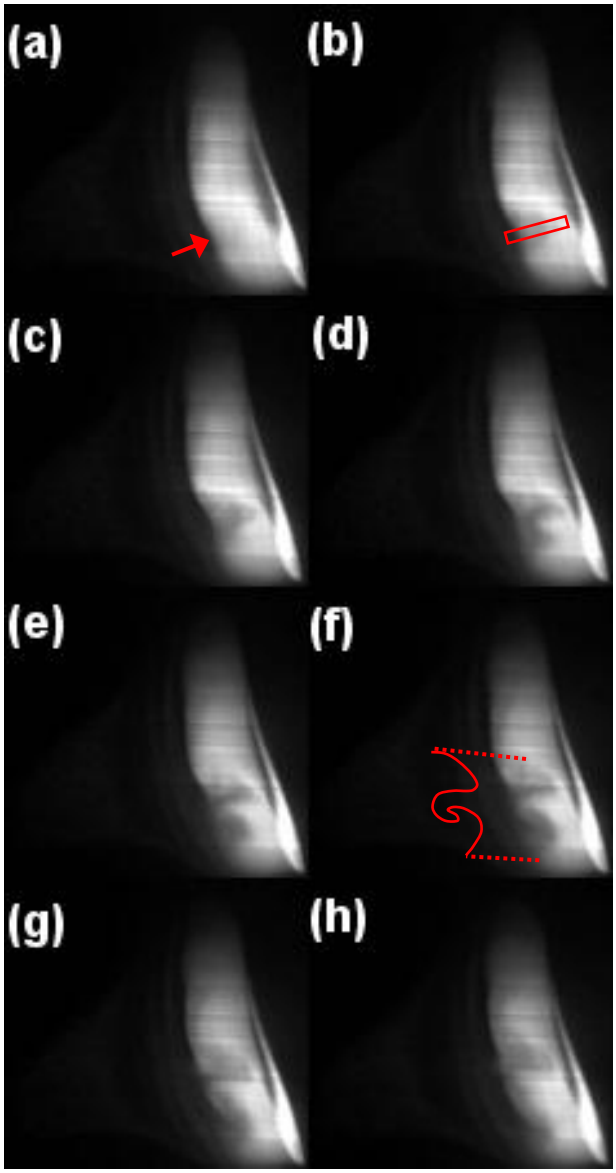

Figure 3

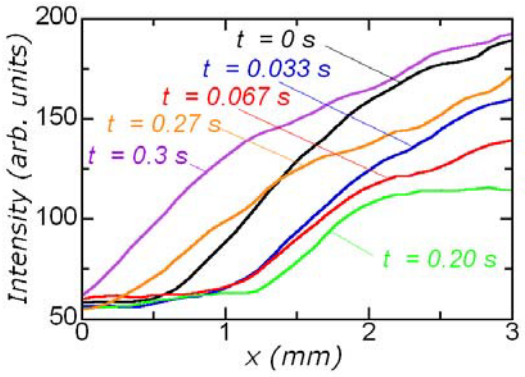
Intensity (arb. units)
200
150
100
50
0
1
2
3
x (mm)
t = 0 s
t = 0.033 s
t = 0.067 s
t = 0.27 s
t = 0.3 s
t = 0.20 s

Figure 4

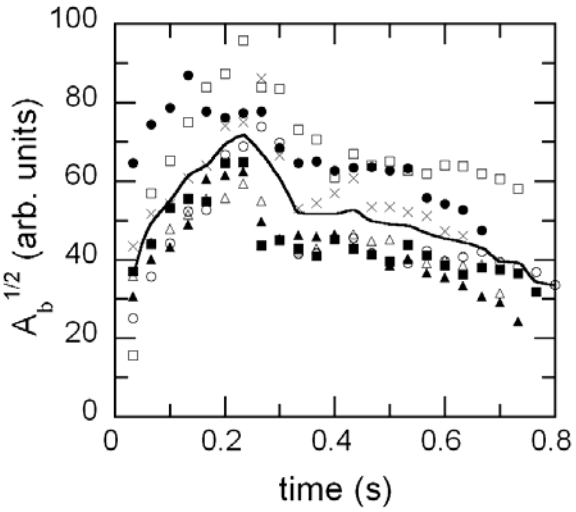

Figure 5